

OPEN

A Two-Component regulatory system with opposite effects on glycopeptide antibiotic biosynthesis and resistance

Rosa Alduina^{1*}, Arianna Tocchetti², Salvatore Costa¹, Clelia Ferraro¹, Patrizia Cancemi¹, Margherita Sosio² & Stefano Donadio²

The glycopeptide A40926, produced by the actinomycete *Nonomuraea gerenzanensis*, is the precursor of dalbavancin, a second-generation glycopeptide antibiotic approved for clinical use in the USA and Europe in 2014 and 2015, respectively. The final product of the biosynthetic pathway is an *O*-acetylated form of A40926 (acA40926). Glycopeptide biosynthesis in *N. gerenzanensis* is dependent upon the *dbv* gene cluster that encodes, in addition to the two essential positive regulators Dbv3 and Dbv4, the putative members of a two-component signal transduction system, specifically the response regulator Dbv6 and the sensor kinase Dbv22. The aim of this work was to assign a role to these two genes. Our results demonstrate that deletion of *dbv22* leads to an increased antibiotic production with a concomitant reduction in glycopeptide resistance. Deletion of *dbv6* results in a similar phenotype, although the effects are not as strong as in the $\Delta dbv22$ mutant. Consistently, quantitative RT-PCR analysis showed that Dbv6 and Dbv22 negatively regulate the regulatory genes (*dbv3* and *dbv4*), as well as some *dbv* biosynthetic genes (*dbv23* and *dbv24*), whereas Dbv6 and Dbv22 positively regulate transcription of the single, cluster-associated resistance gene. Finally, we demonstrate that exogenously added acA40926 and its precursor A40926 can modulate transcription of *dbv* genes but with an opposite extent: A40926 strongly stimulates transcription of the Dbv6/Dbv22 target genes while acA40926 has a neutral or negative effect on transcription of those genes. We propose a model in which glycopeptide biosynthesis in *N. gerenzanensis* is modulated through a positive feedback by the biosynthetic precursor A40926 and a negative feedback by the final product acA40926. In addition to previously reported control systems, this sophisticated control loop might help the producing strain cope with the toxicity of its own product. This work, besides leading to improved glycopeptide producing strains, enlarges our knowledge on the regulation of glycopeptide biosynthesis in actinomycetes, setting *N. gerenzanensis* and its two-component system Dbv6-Dbv22 apart from other glycopeptide producers.

The glycopeptide antibiotic A40926 (Fig. 1A) is the precursor for dalbavancin (Fig. 1B), a semisynthetic lipoglycopeptide clinically used for treatment of acute skin infections caused by methicillin-susceptible and methicillin-resistant *Staphylococcus aureus* and *Streptococcus pyogenes*.

A40926 is produced by the actinomycete *N. gerenzanensis* as a complex of related compounds, differing mostly by the type of *N*-acyl chain attached to the glucuronic acid moiety. The core structure of A40926 consists of a heptapeptide containing the proteinogenic amino acid tyrosine and the non-proteinogenic amino acids 3,5-dihydroxyphenylglycine (DPG) and 4-hydroxyphenylglycine (HPG). The heptapeptide is assembled by a nonribosomal peptide synthetase (NRPS) and modified by the action of various enzymes: four oxygenases, one halogenase, one hydroxylase, two glycosyltransferases, one hexose oxidase, one methyltransferase, one *N*-deacetylase, one *N*-acyltransferase and one *O*-acetyltransferase¹. The form with the acetylated mannose (acA40926) is considered the final biosynthetic product². However, mild extraction conditions are necessary to

¹Department of Biological, Chemical and Pharmaceutical Sciences and Technologies, University of Palermo, Viale delle Scienze, 90128, Palermo, IT, Italy. ²Nacons Srl, Via Ortles 22/4, 20139, Milan, Italy. *email: valeria.alduina@unipa.it

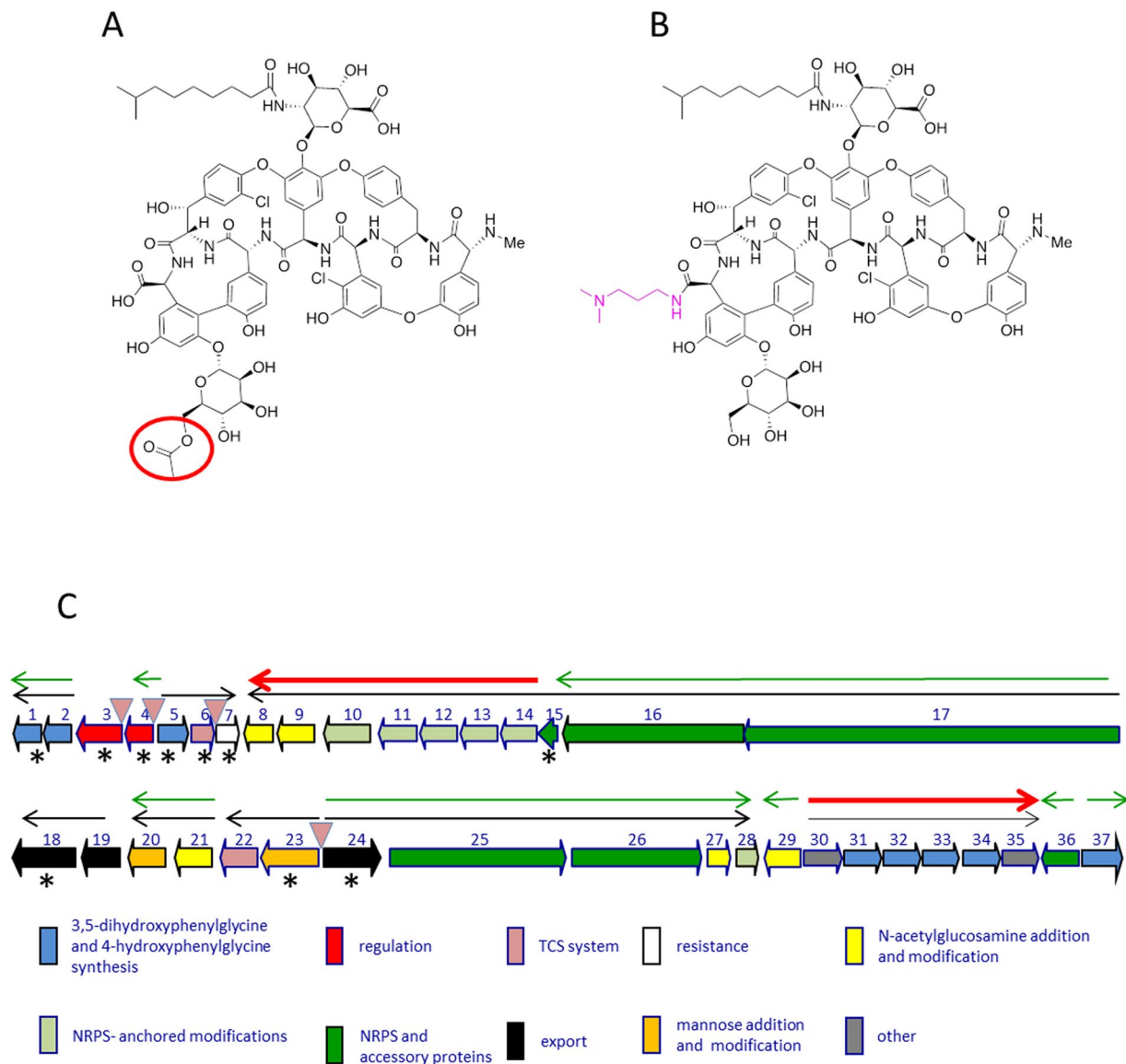


Figure 1. Chemical structures of O-acetyl A40926 (**A**) and of dalbavancin (**B**) and genetic organization of the *dbv* cluster (**C**). (**A,B**) Only the component B0 (the major congener in the A40926 complex) is shown for simplicity. The acetyl group of A40926 and the chemical modification present in dalbavancin are indicated in red circle and pink, respectively. (**C**) The thin black arrows indicate experimentally determined operons. Red and green arrows represent the transcriptional units controlled by Dbv4 and Dbv3, respectively. The *dbv* genes are grouped by functional category as indicated. Asterisks indicate the genes analyzed by qRT-PCR analysis in the present work.

isolate acA40926. While A40926 and acA40926 are equipotent in antibacterial activity against most strains, the former is slightly more active against *S. aureus* and *Neisseria gonorrhoeae*³. Hence, the desacetylated form has been used as the substrate for dalbavancin semi-synthesis. In addition, as many methods for complex analysis involve alkaline treatment of the culture, which results in hydrolysis of the ester bond, past literature considered A40926 as the main fermentation product. Detailed studies of the regulation of glycopeptide biosynthesis in *N. gerzanensis* will be crucial for the development of rational approaches towards overproduction of the dalbavancin precursor. The *dbv* gene cluster for acA40926 biosynthesis contains 37 protein-coding sequences (Fig. 1C) that participate in antibiotic biosynthesis, regulation, immunity, and export^{1,4}. Specifically, the cluster encodes the positive regulators Dbv3 and Dbv4 that indirectly or directly activate different operons leading to acA40926 biosynthesis^{5,6}. Dbv3 and Dbv4 belong to the LAL (large ATP binding regulators of LuxR) and the StrR family of regulators, respectively. The cluster also contains the putative response regulator *dbv6* and the sensor-kinase *dbv22*, whose products may be part of a two-component system (TCS), even if the genes are not organized in a bicistronic operon^{4,7}. A relevant characterized TCS in actinomycetes is the *Streptomyces coelicolor* VanR (VanR_{sc}) and VanS (VanS_{sc}) system associated with a glycopeptide resistance cassette in this species, which however does not produce any glycopeptide.

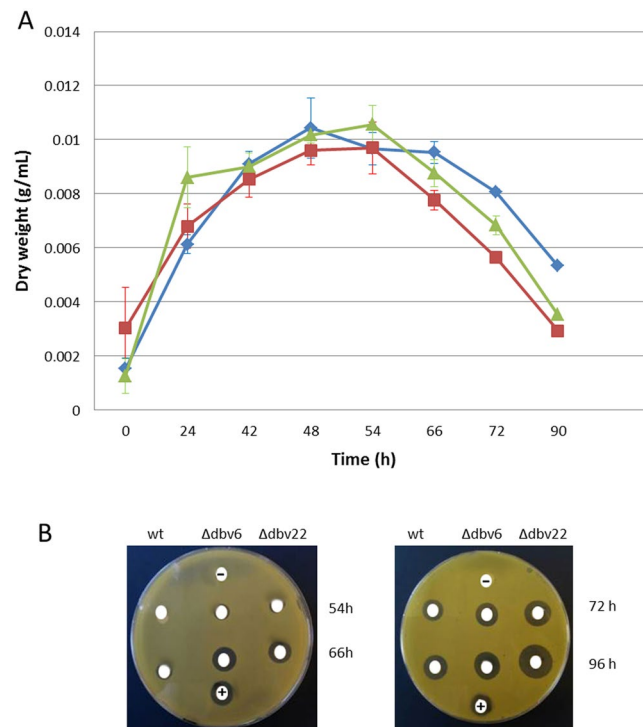


Figure 2. Growth curves and antibiotic production by *N. gerenzanensis* wild type, $\Delta dbv6$ and $\Delta dbv22$ strains in RARE3 medium. **(A)** The dry weight of the wild type, $\Delta dbv6$ and $\Delta dbv22$ strains are shown with green, red and blue lines, respectively. Standard deviation was calculated as average of three technical and two biological replicates. **(B)** Bioassays of 50 μ L of the culture broth of the wild type, $\Delta dbv6$ and $\Delta dbv22$ strains using *K. rhizophila* as test strain. (+) and (-) indicate the positive (culture broth collected from the parental strain after 120 h) and negative (only growth medium) control, respectively.

In *S. coelicolor*, following vancomycin induction, the VanRSsc TCS activates transcription of the *van-HAX* genes, leading to the synthesis of peptidoglycan precursors terminating with D-alanyl-D-lactate (DAla-D-Lac), causing a 1000-fold decreased binding affinity of vancomycin to its target⁸⁻¹¹. Thus, in its induction mechanism and in the resulting peptidoglycan modification, the mechanism leading to glycopeptide resistance in *S. coelicolor* resembles that used by pathogenic *Enterococcus* spp^{12,13}. While some glycopeptide producers do contain a *vanHAX* cassette, either associated with the gene cluster¹⁴⁻¹⁶ or elsewhere in the genome¹⁷, the *N. gerenzanensis* genome does not contain any such genes¹⁸. *N. gerenzanensis* must thus use different strategy(ies) to cope with the self-toxicity of its own product. Marcone and coworkers showed that the wild type strain synthesizes a peptidoglycan with 3-3 cross-linked peptide stems using the carboxypeptidase Dbv7¹⁹. Using substrates mimicking peptidoglycan, it was shown that Dbv7 cuts the D-Ala-D-Ala end of the peptidoglycan precursor on the outer surface of the cell membrane, mainly before and during antibiotic production^{19,20}. However, deletion of *dbv7* in the original host or its heterologous expression result in measurable but modest differences in glycopeptide resistance¹⁹.

In this study, we characterized the function of *dbv6* and *dbv22* with respect to glycopeptide biosynthesis and resistance in *N. gerenzanensis* and established that *dbv* biosynthesis genes are under negative control by this TCS, while the resistance gene *dbv7* is under positive control. In addition, we discovered that exogenously added A40926 and acA40926 differently affect transcription of selected *dbv* genes. Based on the current results and those reported previously², a complex model of regulation can be depicted with the late pathway intermediate A40926 and the end product acA40926 having different roles in controlling antibiotic biosynthesis and resistance.

Results

Dbv6 and Dbv22 are transcriptional repressors of A40926 biosynthesis. *N. gerenzanensis* mutants defective in *dbv6* and *dbv22* were constructed as previously reported⁶ and as described under Material and Methods, respectively. When *N. gerenzanensis* was grown in a rich medium (RARE3) that affords good growth but moderate glycopeptide production, disruption of *dbv6* or *dbv22* did not significantly affect biomass accumulation (Fig. 2A). Interestingly, bioassays (Fig. 2B) of culture broth collected along the growth showed that antibiotic production started at 54 h in both mutants (12 h earlier than in the parental strain) and proceeded to higher levels up to 96 h, the last analyzed time point. Liquid chromatography-mass spectrometry (LC-MS) analysis of 96-h culture broths showed that the $\Delta dbv6$ and $\Delta dbv22$ mutants produced 52 and 70 μ g/mL acA40926, respectively, in comparison with 34 μ g/mL, as observed with the parental strain.

When *N. gerenzanensis* was grown in a production medium (V40P), the higher production levels of the mutants were confirmed, with the $\Delta dbv6$ and $\Delta dbv22$ mutants producing 210 and 354 μ g/mL acA40926 after

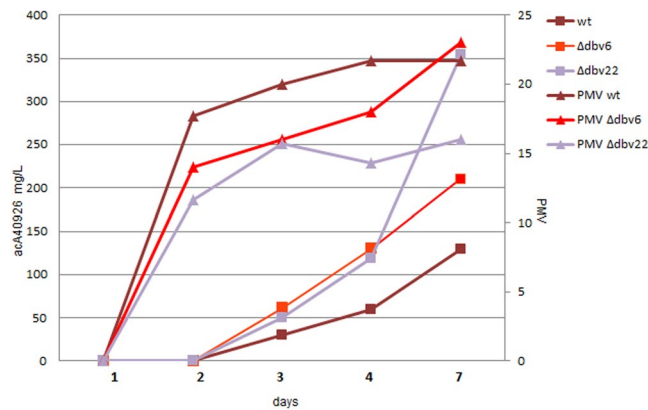


Figure 3. AcA40926 production and growth in V40P medium of the wild type, $\Delta dbv6$ and $\Delta dbv22$ strains. Squares indicate acA40926 concentrations, while triangles represent %PMV. Brown, red and violet symbols correspond to the wild type, $\Delta dbv6$ and $\Delta dbv22$ strains, respectively.

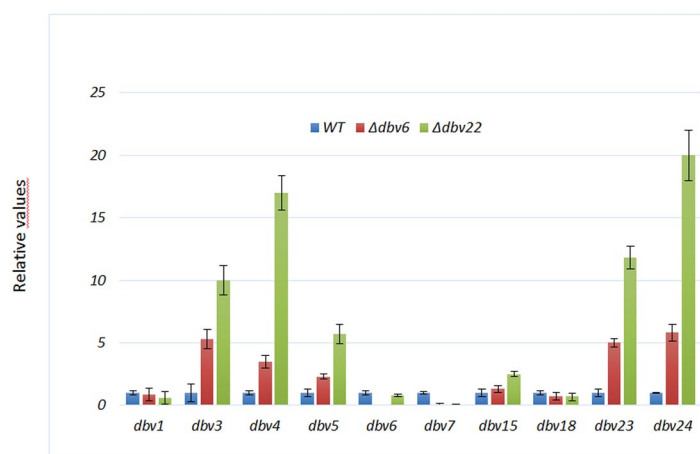


Figure 4. qRT-PCR of *dbv* genes in the wild type and $\Delta dbv6$ and $\Delta dbv22$ mutant strains. For each gene, data are normalized to the parental strain (blue bars). Red and green bars represent relative RNA levels seen in the $\Delta dbv6$ and $\Delta dbv22$ strains, respectively. Error bars are calculated from three independent determinations of mRNA abundance in each sample. RNAs were extracted after 54 h of growth in RARE3 medium.

7 days, respectively, in comparison with 130 $\mu\text{g}/\text{mL}$ seen in the parental strain (Fig. 3). Interestingly, under these conditions, we observed a small but consistent decrease in biomass accumulation, which was inversely related to the amount of produced glycopeptide. There was no difference in complex composition between the mutants and the wild type (Supplementary Fig. S1), with acA40926 as the main product at all time points in the three strains.

These results demonstrate that Dbv6 and Dbv22 negatively regulate glycopeptide production and their abolition leads to increased antibiotic production, despite a small decrease in biomass, indicating a substantial higher productivity of the mutants (in terms of μg of product per unit of biomass) in comparison to the parental strain. Across two different media, deletion of *dbv22* has a more prominent effect than *dbv6*.

Quantitative RT-PCR (qRT-PCR) analysis after 54 h of growth in RARE3 medium of the wild type and the two mutants was carried out to identify the Dbv6/Dbv22 target genes within the *dbv* cluster (Fig. 4). We focused our attention on ten genes as representatives of all the *dbv* operons. Besides the regulators *dbv3*, *dbv4* and *dbv6*, the analysis was carried out on the biosynthetic genes *dbv1* and *dbv5* (HPG synthesis), *dbv23* (mannose acetylation) and *dbv15* (MbtH-like protein assisting NRPS action), on the ABC-transporter genes *dbv18*, and *dbv24*, and on the resistance gene *dbv75,21* (Fig. 1C). Consistent with the results from bioassays and LC-MS analysis, qRT-PCR analysis showed that transcription of some analyzed genes was strongly influenced by deletion of *dbv6* and more so by *dbv22* genes (Fig. 4). Indeed, the transcriptional levels of *dbv3*, *dbv4*, *dbv5*, *dbv23* and *dbv24* increased approximately 2–5 fold in the $\Delta dbv6$ mutant and 5–20 fold in the $\Delta dbv22$ mutant; in contrast, *dbv7* was apparently not transcribed in both mutants. The transcriptional levels of *dbv1*, *dbv6*, and *dbv18* were not influenced by either mutation (Fig. 4).

Dbv22 enhances glycopeptide resistance. We tested the wild type and the two mutant strains for sensitivity to A40926 and acA40926. Consistent with previous results¹⁹, the wild type strain formed no visible colonies when plated on medium containing 4 $\mu\text{g}/\text{mL}$ A40926. Remarkably, it was more sensitive to acA40926 than to its

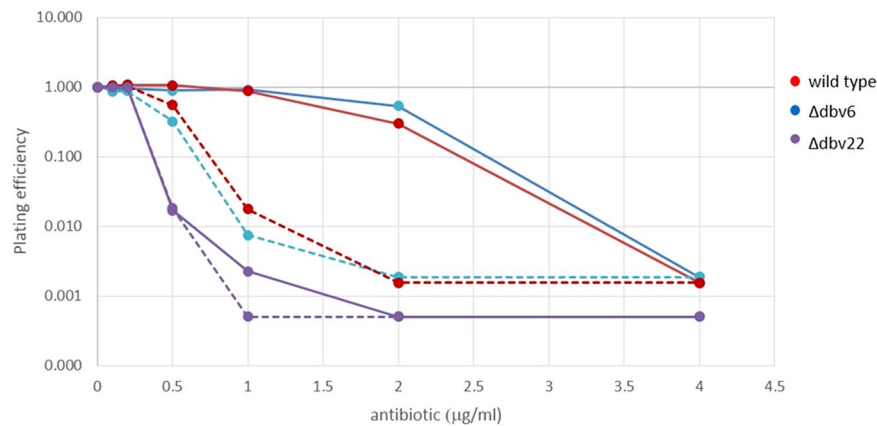


Figure 5. Resistance assay of the wild type and $\Delta dbv6$ and $\Delta dbv22$ mutant strains. Plating efficiency of the wild type, $\Delta dbv6$ and $\Delta dbv22$ strains on different concentrations of A40926 (solid lines) or of acA40926 (dashed lines). Reported data are the average of two independent counts. The limit of detection were 10^5 CFU/mL for the wild type, $\Delta dbv6$, and $\Delta dbv22$ strains.

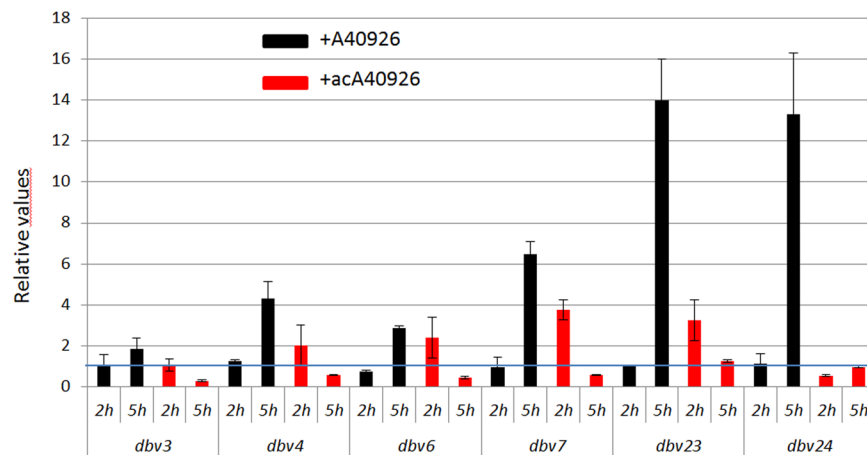


Figure 6. qRT-PCR analysis of the gene expression of *dbv3*, *dbv4*, *dbv6*, *dbv7*, *dbv23* and *dbv24* in the wild type strain. RNA was isolated from the wild type strain incubated in V40P medium for 2 and 5 h in the presence of $0.5 \mu\text{g/mL}$ A40926 (black bars) or $0.5 \mu\text{g/mL}$ acA40926 (red bars). Data are expressed as relative values to the no-addition controls. Within each sample, mRNA levels were normalized to *hrdB*, arbitrarily setting the ratio for each sample to 1. Standard deviations are calculated from three independent determinations of mRNA abundance in each sample.

desacetylated precursor, with a significant reduction in the ability to form colonies observed already at $0.5\text{--}1 \mu\text{g/mL}$ (Fig. 5). No significant differences between the wild type and the $\Delta dbv6$ mutant were observed. In contrast, the $\Delta dbv22$ mutant strain was more sensitive to acA40926 and A40926, and it was able to form visible colonies only with up to 0.5 and $0.2 \mu\text{g/mL}$ of A40926 and acA40926, respectively (Fig. 5). Thus, consistent with qRT-PCR analysis, Dbv22 positively controls resistance to glycopeptides, likely by regulating expression of the carboxypeptidase Dbv7. The lack of an effect on glycopeptide resistance by the *dbv6* deletion might be due to the narrow range of glycopeptide concentration in which an effect is seen.

A40926 strongly induces expression of *dbv* genes. The above results indicate that *N. gerezanensis* can discriminate, in terms of sensitivity, between the highly related glycopeptides A40926 and acA40926. Previous work had also indicated that exogenously added acA40926, but not its desacetylated form, had an inhibitory effect on glycopeptide production². We thus wondered whether exogenously added glycopeptides would have any effect on the transcriptional levels of the Dbv6/Dbv22 target genes. To this end, a 24 h culture of the parental strain in V40P medium was equally divided into three flasks, with each flask receiving either $0.5 \mu\text{g/mL}$ A40926, $0.5 \mu\text{g/mL}$ acA40926 or no addition. After further 2- and 5-h incubation, RNA was extracted and the transcriptional levels of all the regulatory genes (*dbv3*, *dbv4* and *dbv6*) and of the Dbv6-targeted genes (*dbv7*, *dbv23* and *dbv24*) were analyzed by qRT-PCR (Fig. 6). Addition of acA40926 had a modest inducing effect on the expression of the regulatory genes *dbv4* and *dbv6*, the resistance gene *dbv7* and the acetyltransferase gene *dbv23*, but only 2 h after compound addition. After 5 h, genes were slightly repressed (*dbv3*, *dbv4*, *dbv6* and *dbv7*) or unaffected (*dbv23* and

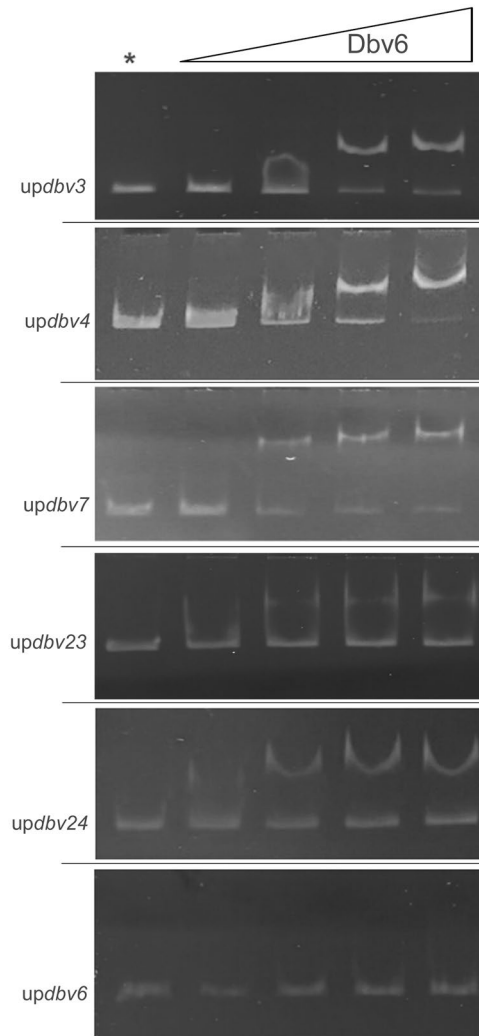


Figure 7. Gel mobility shift assays of DNA regions upstream of *dbv3*, *dbv4*, *dbv7*, *dbv23*, *dbv24* and *dbv6*. Lanes labeled with an asterisk contained the probe only (up*dbv3*, up*dbv4*, up*dbv7*, up*dbv23*, up*dbv24* and up*dbv6*). All lanes contained 50 ng of target DNA. Increasing concentrations of His-Dbv6 (0.5, 1, 1.5, 2 mM) were incubated in the presence of probes as indicated.

dbv24). In contrast, addition of A40926 did not significantly affect transcription levels after 2 h. However, after 5 h all the analyzed genes were induced, with transcription levels 2-fold (for *dbv3*), 3–6-fold (for *dbv4*, *dbv6* and *dbv7*) or 13–14-fold (for *dbv23* and *dbv24*) higher relative to uninduced cells. qRT-PCR of the analyzed *dbv* genes in all three cultures before induction indicated modest flask-to-flask variation (Supplementary Fig. S2).

The above experiments were performed using the wild type strain, which does produce acA40926 and related pathway intermediates, with exogenous compounds added during early exponential growth, when glycopeptide levels are below the limit of detection (about 1 µg/mL). When a similar experiment was carried out with the Δ *dbv4* mutant strain, which does not produce any glycopeptide⁶, we could not detect any transcription of *dbv23* and *dbv24*, suggesting that these genes might be indirect targets of Dbv4 (Supplementary Fig. S3). Thus, one or more components of the glycopeptide complex or intermediates thereof could exert a positive feedback on the transcription of at least some *dbv* genes.

Direct control of Dbv6 on *dbv4* and *dbv7* gene expression. We investigated whether Dbv6 can bind to the upstream region of the target genes and directly control their expression. Gel mobility shift assays of the regions upstream to *dbv3*, *dbv4*, *dbv6*, *dbv7*, *dbv23* and *dbv24* were carried out using a purified His-tagged Dbv6 protein overexpressed in *E. coli*. These assays did reveal a binding activity of Dbv6 towards the upstream regions of the regulatory genes *dbv3* and *dbv4*, of the resistance gene *dbv7*, of the genes *dbv23*–*dbv22*, coding for the acetyltransferase and the sensor kinase, and of the operon *dbv24*–*dbv28*, which encodes an ABC-transporter, two NRPS modules, the *N*-methyltransferase and the enzyme involved in β -hydroxylation of the tyrosine residue (Fig. 7). No shift was detected using the upstream region of *dbv6* (Fig. 7). Control experiments using the internal region of the vegetative sigma factor encoding gene (Supplementary Fig. S4) further confirmed the specificity of

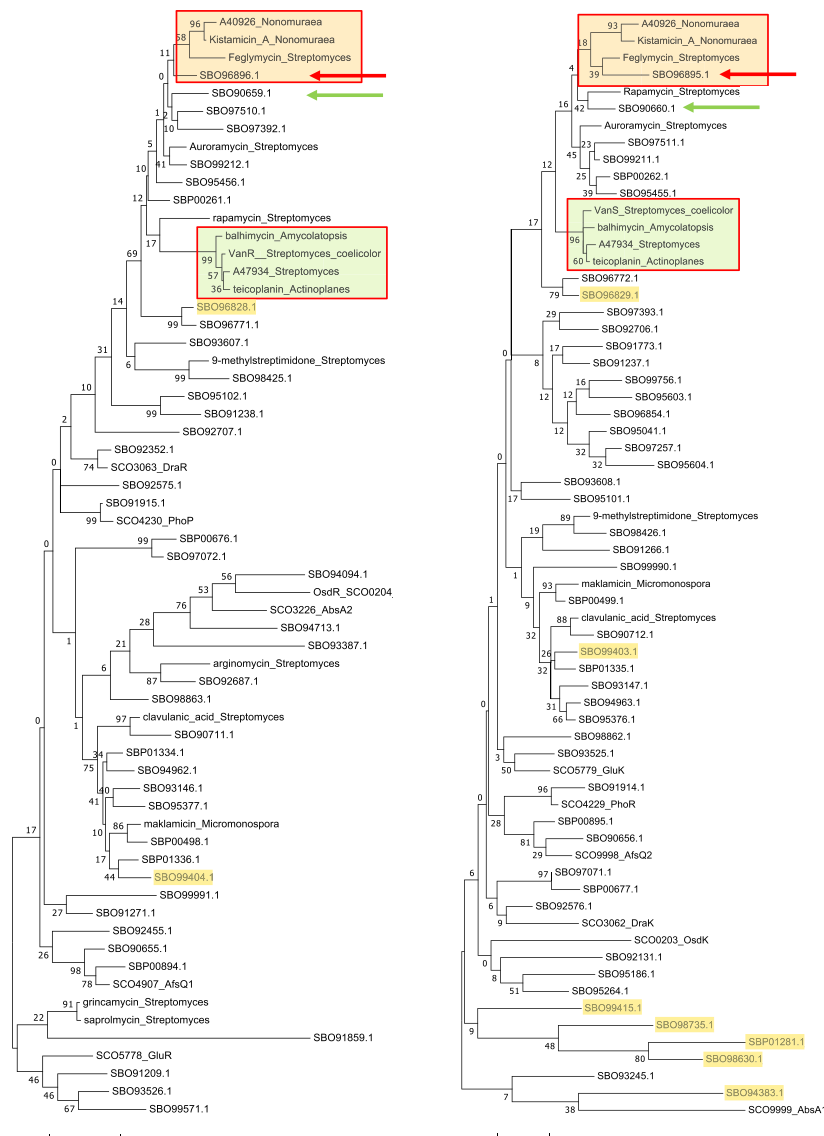


Figure 8. Phylogenetic analysis of 62 response regulators (left panel) and 65 sensory kinases (right panel). Sequences associated with established gene clusters are identified by the compound name followed by the genus of the corresponding strain; characterized *S. coelicolor* proteins are identified by the protein name followed by the SCO code; and *N. gerenzanensis* sequences are denoted by the SBO or SBP codes. The branches associated with the Van- and Dbv-related TCSs are identified by green and orange boxes, respectively. Green and red arrows indicate the adjacent members of two different, uncharacterized *N. gerenzanensis* TCSs closely associated with the Dbv branches. Sequences associated with *N. gerenzanensis* biosynthetic gene clusters, as identified by AntiSMASH 5.0⁴², have a yellow highlight.

DNA binding by Dbv6 observed on some of the target genes. Thus, these data are consistent with Dbv6 directly controlling expression of the target genes. Further studies will be necessary to understand how Dbv6 exerts positive and negative control on different DNA regions.

Dbv6 and Dbv22 are unrelated to other TCSs associated with other glycopeptide gene clusters.

TCSs are often associated with glycopeptide gene clusters, where they have been shown in some cases to play a role in glycopeptide resistance. They appear similar to the well-characterized *S. coelicolor* VanRS system, which plays a role in glycopeptide resistance in a non-producing strain⁹. However, reciprocal Blast searches indicate that Dbv6 and Dbv22 are not orthologs of VanR_{sc} and VanS_{sc}, respectively. Inspired by recent work on phylogenetic analysis of cluster-associated StrR- and LuxR-related regulators²², we performed a phylogenetic analysis of TCSs from actinomycetes. To this end, we retrieved response regulators and sensory kinases associated with characterized actinobacterial gene clusters from the MiBIG database²³, well-characterized TCSs from *Streptomyces coelicolor*^{24,25} and the response regulators and sensory kinases identified in the *N. gerenzanensis* genome¹⁸ (Fig. 8).

With respect to the response regulators, those associated with the balhimycin, teicoplanin and A47934 clusters branch together along with *S. coelicolor* VanR (Fig. 7, left panel). In contrast, Dbv6 clusters together with response

Strain or plasmid	Description	Source or reference
Bacterial strains		
<i>Nonomuraea gerenzanensis</i>	Wild type	ATCC 39727
$\Delta dbv6$ mutant	<i>N. gerenzanensis</i> strain in which the <i>dbv6</i> gene was replaced with an apramycin cassette	6
$\Delta dbv22$ mutant	<i>N. gerenzanensis</i> strain in which the <i>dbv22</i> gene was replaced with an apramycin cassette	This study
<i>Kocuria rhizophila</i>	Used for bioassay of A40926	ATCC 9341
<i>Escherichia coli</i> DH10B	F_ <i>endA1 recA1 galE15 galK16 nupG rpsL</i> $\Delta lacX74$ $\Delta 80lacZ\Delta M15$ <i>araD139</i> Δ (<i>ara-leu</i>)7697 <i>mcrA</i> Δ (<i>mrr-hsdRMS-mcrBC</i>) λ ; host for routine subcloning experiments	Invitrogen
<i>Escherichia coli</i> ET12567/pUZ8002	(<i>dam-13::Tn9 dcm-6</i>) pUZ8002 ⁺ ($\Delta oriT$); used for conjugative transfer of DNA and for demethylating plasmid DNA	44
<i>Escherichia coli</i> BW25113/pIJ790	Δ (<i>araD-araB</i>)567 $\Delta lacZ4787$ (<i>::rrnB-4</i>) <i>lacIp-4000</i> (<i>lacIq</i>) λ <i>rpoS369</i> (Am) <i>rph-1</i> Δ (<i>rhaD-rhaB</i>) 568 <i>hsdR514</i> ; used to generate recombinant cosmid 1B1	45
Plasmid/cosmid		
1B1	Cosmid containing part of the <i>dbv</i> cluster from <i>dbv17</i> to <i>dbv37</i>	4
1B1 $\Delta dbv22$	Derivative of 1B1 with the inactivated <i>dbv22</i> gene	This study
pIJ773	pUC19 containing the <i>aac(3)IV-oriT</i> cassette; source of the <i>aac(3)</i> gene	37

Table 1. Bacterial strains, plasmids and cosmids used in this study.

regulators associated with gene clusters for kistamicin A (from a *Nonomuraea* sp²⁶) and for feglymycin (from a *Streptomyces* sp²⁷). Kistamicin A is a partially cross-linked heptapeptide sharing some amino acid residues with glycopeptide antibiotics, whereas feglymycin is a linear tridecapeptide containing several HPG and DPG residues. Both compounds have antiviral activity but modest antibacterial activity in comparison with glycopeptide antibiotics^{28–30}.

A similar picture emerges when analyzing the sensory kinases: those associated with the balhimycin, teicoplanin and A47934 clusters, and *S. coelicolor* VanS form a separate branch from the one containing Dbv22 and the kistamicin A- and feglymycin-associated sequences (Fig. 8, right panel). Interestingly, the adjacent members of two different, uncharacterized TCSs encoded by the *N. gerenzanensis* genome cluster closely with the Dbv6 and Dbv22 branches, suggesting these proteins might respond to similar stimuli and/or be regulated by similar factors. It should be noted that all the other sensory kinases or response regulators from *N. gerenzanensis* associated to a putative biosynthetic gene cluster are unrelated to Dbv6 or Dbv22.

Discussion

The results presented here provide evidence that the response regulator Dbv6 and the sensor kinase Dbv22 negatively control A40926 production and that Dbv22 positively controls A40926 resistance. These effects are associated with altered transcription levels. Indeed, strains deleted for these genes are upregulated in the expression of the two key regulators *dbv3* and *dbv4*. Conversely, the $\Delta dbv22$ mutant strain expresses less *dbv7*, the only resistance gene present in the *dbv* cluster. This would suggest that Dbv6 and Dbv22 represent the two components of a signal transduction system responding to some stimuli and controlling key elements of the *dbv* cluster. Remarkably, deletion of *dbv22* can lead to the paradoxical result of a mutant producing increased glycopeptide levels while becoming more sensitive to its own product.

While TCSs are frequently found in glycopeptide gene clusters, different regulatory strategies are apparently adopted by glycopeptide-producing actinomycetes. Abolition of the response regulator or of the sensor kinase gene in *Streptomyces toyocaensis* led to increased sensitivity to A47934¹¹. In *Amycolatopsis balhimycina*, the deletion of genes for the VanRS-like TCS VnRSAb affected VanY expression in a $\Delta vanHAX$ background³¹ while did not influence balhimycin production^{17,31}. In the glycopeptide non-producing *S. coelicolor*, deletion of *vanR* but not of *vanS* led to a strain sensitive to vancomycin¹¹. Apart from the VanR genes associated with a *vanHAX* resistance cassette (e.g. those from *S. coelicolor*, *S. toyocaensis* and *Actinoplanes teichomyceticus*), the gene(s) targeted by VanR in *A. balhimycina* remain to be identified. Here, we demonstrate that in *N. gerenzanensis* direct target genes of Dbv6 are the regulatory genes *dbv3* and *dbv4*, and the genes *dbv23-dbv22*, coding for the acetyltransferase and the sensor kinase, and the *dbv24-dbv28* operon, since the transcription of all these genes is induced in the $\Delta dbv6$ mutant background and that Dbv6 binds to the upstream regions of these genes. Another direct target of Dbv6 but regulated in the opposite manner is the peptidase *dbv7* (Fig. 7).

The impacts of the *dbv6* and *dbv22* mutations are quantitatively different. First of all, the relative expression levels of the analyzed *dbv* genes (encoding the positive regulators Dbv3 and Dbv4, the prephenate dehydrogenase Dbv5, the acetyltransferase Dbv23 and the ABC-transported Dbv24) in the $\Delta dbv6$ mutant are somehow intermediate between those of the parental strain and of the $\Delta dbv22$ mutant (Fig. 4). In terms of antibiotic resistance, the $\Delta dbv22$ strain is marginally but consistently more sensitive than the parental strain and the $\Delta dbv6$ mutant to A40926 and acA40926. Finally, when *N. gerenzanensis* is grown in production medium, the $\Delta dbv6$ and the $\Delta dbv22$ mutants show, up to 48 h, an identical but slightly higher acA40926 production rate than the parental strain, with $\Delta dbv22$ keeping an equivalent rate up to 7 days and reaching acA40926 levels (350 $\mu\text{g}/\text{mL}$) significantly higher than $\Delta dbv6$ and the parental strain (200 and 130 $\mu\text{g}/\text{mL}$, respectively; Fig. 3). Remarkably, higher production levels by $\Delta dbv22$ are achieved despite a slightly lower biomass accumulation (Fig. 3).

Gene(s)	Forward (5'-3')	Reverse (5'-3')	Predicted size (bp)
Used in RT-PCR or qRT-PCR			
<i>hrdb</i>	ctgatcaacaaggtcgccc	gccgtacctctgcacctcg	129
<i>16S</i>	agcttggtggggtagtg	tcaccgtacaccaggaatt	470
<i>dbv3</i>	gaagaggtgccagggtcac	ccgaggcgctctacatcac	101
<i>dbv4</i>	cagtaattccggcttggtcc	aaacaggtcgcatctccc	114
<i>dbv5</i>	gtggacctggcattgatcg	ctggtcacatcgggtgtacgc	101
<i>dbv6</i>	agctgtgcgctgagatcg	acggcttcggcagatagtc	126
<i>dbv7</i>	ccagctcgtcggtctcac	cccttgacgtggtggac	141
<i>dbv23</i>	gaccgccactgttgatc	ggcagctcaccacctacg	110
<i>dbv24</i>	tcggaggtttgctaagg	agatcgaatccaatcgcg	147
Used to prepare probes for EMSA			
<i>upstream 3</i>	gaatcgagcaacctcgtcag	gcaggaatgggaaaggatct	300
<i>upstream 4</i>	gcatcggcttatccgaaac	cgctcgcctcttttcttc	226
<i>upstream 6</i>	tggtcgaggtctccgtgc	cattcgtcgcctcttc	150
<i>upstream 7</i>	tgaaggcgacatcaacc	tcctcatcctctctccag	188
<i>upstream 23</i>	gtccagggtgaacgttggt	ccttcagcaaacctccgaac	178
<i>upstream 24</i>	gcaggctggaaggacatc	gtgaccaagcgttcacctgg	176

Table 2. Primers used in this study.

The fact that all the analyzed parameters are more strongly altered in the $\Delta dbv22$ than in the $\Delta dbv6$ background suggests that Dbv22 and/or Dbv6 might interact with other response regulators and/or sensor kinases, respectively, present in the cell. Indeed, the *N. gerenzanensis* genome harbors 43 and 47 TCS pairs, some of them highly related to VanR and VanS (Fig. 8). A homologous of *dbv6* gene is present in the *N. gerenzanensis* genome. The gene is located about 4.5 Mbp away from Dbv6, with which it shows 68% sequence identity and 77% similarity. All 8 diagnostic residues of the phosphorylation site are invariant with Dbv6. The HTH domain is highly conserved.

Marcone and coworkers¹⁹ have previously shown that *N. gerenzanensis* is essentially sensitive to A40926, that the carboxypeptidase VanY (i.e., Dbv7) provides some protection but that insensitivity to glycopeptides is mostly acquired during growth by some unknown mechanism. That some other resistance mechanism operates in *N. gerenzanensis* is consistent with our observed lack of transcription of *dbv7* in the $\Delta dbv6$ strain (Fig. 4), a mutant that is as glycopeptide resistant as the parental strain (Fig. 5). Thus, *dbv6* does not apparently contribute to glycopeptide resistance while *dbv22* does, suggesting that a second resistance mechanism influenced by Dbv22 takes over. The complex interplay of glycopeptide production and resistance is also highlighted by the fact that deletion of *dbv7* did not affect A40926 production, as reported by Marcone and coworkers¹⁹.

When added just at 24 h of growth, when no glycopeptide production is detected yet, 0.5 $\mu\text{g}/\text{mL}$ A40926 can strongly induce expression of all tested *dbv* genes, particularly *dbv23* and *dbv24*. AcA40926 has the opposite effect. The simplest explanation of this observation is that A40926, but not acA40926, binds to a receptor to activate signal transduction, relieving inhibition or leading to a massive transcription of *dbv* genes. It is tempting to speculate that the receptor that A40926 binds to is actually Dbv22. Indeed, the ~ 14 -fold stimulation of *dbv24* upon A40926 addition is remarkably similar to its upregulated expression in the $\Delta dbv22$ background. Sensor kinases have been shown to be able to recognize and respond to glycopeptides: VanS_{sc} is induced by vancomycin but not by teicoplanin and A47934^{8,11}, while the *S. toyocaensis* VanS sensor kinase is induced by A47934 but not by vancomycin and teicoplanin¹¹.

In earlier work, we showed that a strain defective in mannose acetylation produces increased levels of A40926 in comparison to the wild type and that this enhanced production can be reverted by adding acA40926 – but not A40926 – to the culture at time zero, while addition of acA40926 had no effect on the wild type². The present and previous results are consistent assuming that acA40926 can also bind to the same receptor but it cannot trigger its activation. Thus, acA40926 would compete with A40926 for the same binding site, acting as an apparent inhibitor of glycopeptide production. Discrimination between the acetylated and desacetylated form of the glycopeptide by *N. gerenzanensis* can also be observed in the resistance profile of the wild type, which is more sensitive to acA40926 than A40926 (Fig. 5).

The data presented here and in previous work^{2,5,6} allow us to refine a possible model for regulation of glycopeptide production in *N. gerenzanensis*¹. When cells are actively growing, transcription of *dbv3* and *dbv4* is repressed by the direct action of Dbv6, as well as by other factors related to growth (nutritional factors, or quorum sensing systems could control A40926 biosynthesis)⁵. At the same time, the resistance gene *dbv7* is expressed as a safeguard mechanism against small amounts of glycopeptides that might be produced. As growth slows down, expression of the master regulators Dbv3 and Dbv4 increases so that some glycopeptide synthesis can occur. When sufficient A40926 accumulates, repression mediated by Dbv6/Dbv22 is relieved and further expression of the *dbv* genes can occur, including that of the acetyltransferase *dbv23* and of the ABC transporter *dbv24*, which results in formation of acA40926 form and its export outside of the cell, where it can compete out A40926 for Dbv22 binding, eventually restoring repression exerted by Dbv6/Dbv22.

This mechanism is somehow reminiscent of the feed forward mechanism proposed for microbisporicin/NAI-107 production in *Microbispora corallina*, where a late pathway intermediate can activate production³² through

the activation of the ECF sigma factor σ^{MibX} , sequestered at the membrane level by an antisigma factor. An unknown signal should lead to production of microbisporicin, the inactivation of the anti-sigma factor, the release of σ^{MibX} , and high-level expression of the entire gene cluster. Interestingly, both A40926 and NAI-107 target lipid II³³, are produced by two strains belonging to different genera of the order *Streptosporangiales* that contain 3–3 cross-linked dimers in their cell wall and that are highly sensitive to their own product³³.

Material and methods

Bacterial strains and culture conditions. The bacterial strains and plasmids used in this study are listed in Table 1. *Escherichia coli* strains were grown in Luria broth liquid medium at 37 °C and supplemented with 50 $\mu\text{g}/\text{mL}$ apramycin when necessary to maintain plasmids.

Cell stocks of the *N. gerenzanensis* strains were prepared from cultures in RARE3 medium as already described³⁴ and stored at -80°C . Liquid cultures were prepared by inoculating 0.2 mL of the frozen stock into 20 mL of RARE3 medium; after 120 h of growth, 1 mL of this culture was inoculated into 50 mL of fresh RARE3 medium in an orbital shaker (500 \times g) in 250-mL baffled flasks at 30 °C. To detect glycopeptide production, samples of culture broths at different time points were withdrawn and stored at -80°C before analysis. Cultivation in glycopeptide production medium was performed as already described². Biomass was determined by measuring the cell dry weight of mycelial pellet recovered from a 1-mL culture sample after drying the pellet at 65 °C for about 24 h. Alternatively, the relative packed mycelial volume (%PMV) was determined after centrifugation of a 6-mL culture sample for 10 min at 4000 \times g.

For assessing induction by glycopeptides, the parental strain or the Δdbv4 mutant were cultivated in V40S medium as above and then transferred into (fresh) V40P medium². After 24 h at 30 °C, the culture was equally divided into three flasks, and either 0.5 $\mu\text{g}/\text{mL}$ A40926 or 0.5 $\mu\text{g}/\text{mL}$ acA40926 were added, with the third flask used as no-addition control. After further 2 and 5 h, 1-mL samples were collected and centrifuged to recover cells. RNA was extracted and processed as below.

Analysis of antibiotic production. Antibiotic production of the mutant strains was firstly evaluated using the paper disc diffusion method and *Kocuria rhizophila* as the assay organism as described previously³⁵. For high-performance liquid chromatography (HPLC) and liquid chromatography-mass spectrometry (LC-MS) analyses, 500 μL aliquots of broth cultures were collected at the time points indicated and treated as reported previously^{6,36}.

Construction of the Δdbv22 strain. PCR targeting³⁷ was applied to replace *dbv22* with a cassette containing an apramycin-selectable marker using pIJ773 as template and the PCR primers reported in Table 2. *E. coli* BW25113/pIJ790 bearing cosmid 1B1⁴ was electrotransformed with the deletion cassette. Intergenic conjugation was carried out as previously reported⁶. Exconjugants were analyzed by PCR (Supplementary Fig. S5) using primers reported in Table 2. One out of eleven clones analyzed contained the interrupted *dbv22* gene and used for further studies. Sequencing of the PCR product confirmed that the apramycin-resistant cassette was correctly inserted in the target gene through homologous double-cross recombination.

Resistance assay. The ability to form colonies of the *N. gerenzanensis* wild type, Δdbv6 and Δdbv22 strains was assessed by plating serial dilutions of stock cultures (prepared from frozen mycelium) on 0.25X BTT plates³⁸ containing 0, 0.1, 0.2, 0.5, 1.0, 2.0 or 4.0 $\mu\text{g}/\text{mL}$ A40926 or acA40926. Two replicate plates were used for each antibiotic concentration. After 6 days at 30 °C, the number of colony forming units (CFU) was recorded.

Total RNA isolation and qRT-PCR analysis. To perform transcriptional analysis, a 6-mL sample was withdrawn from a 30-mL culture. The mycelium was harvested by centrifugation and RNA was extracted using the RNeasy midi kit (Qiagen), followed by treatment with DNase I (Roche) according to the manufacturer's instructions. RNA quality was previously checked using Reverse transcription (RT)-PCR analysis as previously described³⁹. It was converted to cDNA as already described³⁴ and amplified using primers reported in Table 2. As control genes, *hrdB*, encoding a vegetative sigma factor, or 16S rRNA, were used. Gene expression was analyzed quantitatively by using the 7300 real-time PCR system (Applied Biosystems) with SYBR green PCR master mix (Applied Biosystems) in 96-well plates. Two microliters of cDNA was added to 20 μL of the PCR mixture. Amplification required activation of AmpErase UNG at 50 °C for 2 min, followed by denaturation at 95 °C for 10 min and then 40 cycles at 95 °C for 15 s and 60 °C for 1 min.

Overexpression and purification of recombinant protein His-Dbv6. *Escherichia coli* DH10B and BL21 (Invitrogen) were used in this study. Plasmids pGEM-T (Promega) and pRSETB (Invitrogen) were used for cloning PCR products, and protein expression, respectively. *N. gerenzanensis* chromosomal DNA was used as template to amplify *dbv6* by PCR using the primers 5'-aaaaggatccaatgcgcttctggtgga-3' and 5'-ttttaagcttcagatcgatccctcgc-3' (underlines indicate the *Bam*HI and *Hind*III sites, respectively). The amplified fragment was digested with *Bam*HI plus *Hind*III and ligated into the *Bam*HI and *Hind*III sites of pRSETB, yielding pRSET-Dbv6, which was introduced into BL21(DE3)pLysS cells by heat shock treatment⁴⁰. Plasmid pRSET-Dbv6 expresses the entire Dbv6 protein with a His6 tag at its N terminus under the control of the T7 promoter and the *lac* operator. Fidelity of PCR amplification was confirmed by DNA sequencing. Dbv6 overexpression and purification were performed using the procedures already described for Dbv4⁵.

Gel mobility shift assay. The gel mobility shift assay was performed according to the method already described⁴¹. Briefly, for the binding assay, increasing amount of Dbv6 (2.8 to 14 μg) was incubated for 10 min at 4 °C in 20 μL of 12.5 mM Tris-HCl (pH 7.5), 10% glycerol, 62.5 mM KCl, 0.75 mM DTT, and 5 mM MgCl₂. After 15 min of incubation with 100 ng of DNA, complexes and free DNA were resolved on non-denaturing 5%

polyacrylamide gels run in 0.5 × Tris-borate-EDTA buffer at 150 V for approximately 2 h and then stained in a bath containing ethidium bromide. The DNA probes were amplified by PCR using the primers listed in Table 2. BSA and the internal region of *hrdB* were used in control experiment (Supplementary Fig. 4).

Phylogenetic analysis. Thirteen response regulators and ten sensory kinases were retrieved from the MiBIG database of characterized actinobacterial biosynthetic gene clusters²³; and forty-one response regulators and forty-seven sensory kinases were identified by blast searches of the *N. gerenzanensis* genome¹⁸. Seven characterized TCSs from *S. coelicolor* (AbsA, Afs, Dra, Glu, Osd, Pho and Van)^{24,25} were also included. Sequences associated with *N. gerenzanensis* biosynthetic gene clusters were identified by AntiSMASH 5.0⁴². Sequence alignments and phylogenetic analyses were performed with the MEGA 7 package⁴³.

Received: 20 November 2019; Accepted: 3 March 2020;

Published online: 10 April 2020

References

1. Alduina, R., Sosio, M. & Donadio, S. Complex Regulatory Networks Governing Production of the Glycopeptide A40926. *Antibiotics* **7**, <https://doi.org/10.3390/antibiotics7020030> (2018).
2. Sosio, M., Canavesi, A., Stinchi, S. & Donadio, S. Improved production of A40926 by *Nonomuraea* sp. through deletion of a pathway-specific acetyltransferase. *Applied microbiology and biotechnology* **87**, 1633–1638, <https://doi.org/10.1007/s00253-010-2579-2> (2010).
3. Goldstein, B. P. *et al.* A40926, a new glycopeptide antibiotic with anti-*Neisseria* activity. *Antimicrobial agents and chemotherapy* **31**, 1961–1966 (1987).
4. Sosio, M., Stinchi, S., Beltrametti, F., Lazzarini, A. & Donadio, S. The gene cluster for the biosynthesis of the glycopeptide antibiotic A40926 by *nonomuraea* species. *Chem Biol* **10**, 541–549 (2003).
5. Alduina, R. *et al.* Phosphate-controlled regulator for the biosynthesis of the dalbavancin precursor A40926. *Journal of bacteriology* **189**, 8120–8129, <https://doi.org/10.1128/JB.01247-07> (2007).
6. Lo Grasso, L. *et al.* Two Master Switch Regulators Trigger A40926 Biosynthesis in *Nonomuraea* sp. Strain ATCC 39727. *Journal of bacteriology* **197**, 2536–2544, <https://doi.org/10.1128/JB.00262-15> (2015).
7. Donadio, S., Sosio, M., Stegmann, E., Weber, T. & Wohlleben, W. Comparative analysis and insights into the evolution of gene clusters for glycopeptide antibiotic biosynthesis. *Molecular genetics and genomics: MGG* **274**, 40–50, <https://doi.org/10.1007/s00438-005-1156-3> (2005).
8. Hong, H. J. *et al.* Characterization of an inducible vancomycin resistance system in *Streptomyces coelicolor* reveals a novel gene (*vanK*) required for drug resistance. *Molecular microbiology* **52**, 1107–1121, <https://doi.org/10.1111/j.1365-2958.2004.04032.x> (2004).
9. Hutchings, M. I., Hong, H. J. & Buttner, M. J. The vancomycin resistance VanRS two-component signal transduction system of *Streptomyces coelicolor*. *Molecular microbiology* **59**, 923–935, <https://doi.org/10.1111/j.1365-2958.2005.04953.x> (2006).
10. Hong, H. J., Hutchings, M. I. & Buttner, M. J. Biotechnology & Biological Sciences Research Council, U. K. Vancomycin resistance VanS/VanR two-component systems. *Advances in experimental medicine and biology* **631**, 200–213, https://doi.org/10.1007/978-0-387-78885-2_14 (2008).
11. Novotna, G. B., Kwun, M. J. & Hong, H. J. *In Vivo* Characterization of the Activation and Interaction of the VanR-VanS Two-Component Regulatory System Controlling Glycopeptide Antibiotic Resistance in Two Related *Streptomyces* Species. *Antimicrobial agents and chemotherapy* **60**, 1627–1637, <https://doi.org/10.1128/AAC.01367-15> (2015).
12. Haldimann, A., Fisher, S. L., Daniels, L. L., Walsh, C. T. & Wanner, B. L. Transcriptional regulation of the *Enterococcus faecium* BM4147 vancomycin resistance gene cluster by the VanS-VanR two-component regulatory system in *Escherichia coli* K-12. *Journal of bacteriology* **179**, 5903–5913, <https://doi.org/10.1128/jb.179.18.5903-5913.1997> (1997).
13. Arthur, M., Molinas, C. & Courvalin, P. The VanS-VanR two-component regulatory system controls synthesis of depsipeptide peptidoglycan precursors in *Enterococcus faecium* BM4147. *Journal of bacteriology* **174**, 2582–2591, <https://doi.org/10.1128/jb.174.8.2582-2591.1992> (1992).
14. Sosio, M. *et al.* Organization of the teicoplanin gene cluster in *Actinoplanes teichomyeticus*. *Microbiology* **150**, 95–102, <https://doi.org/10.1099/mic.0.26507-0> (2004).
15. Li, T. L. *et al.* Biosynthetic gene cluster of the glycopeptide antibiotic teicoplanin: characterization of two glycosyltransferases and the key acyltransferase. *Chem Biol* **11**, 107–119, <https://doi.org/10.1016/j.chembiol.2004.01.001> (2004).
16. Pootoolal, J. *et al.* Assembling the glycopeptide antibiotic scaffold: The biosynthesis of A47934 from *Streptomyces toyocaensis* NRRL15009. *Proc Natl Acad Sci USA* **99**, 8962–8967, <https://doi.org/10.1073/pnas.102285099> (2002).
17. Schaberle, T. F. *et al.* Self-resistance and cell wall composition in the glycopeptide producer *Amycolatopsis balhimycina*. *Antimicrobial agents and chemotherapy* **55**, 4283–4289, <https://doi.org/10.1128/AAC.01372-10> (2011).
18. D'Argenio, V. *et al.* The complete 12 Mb genome and transcriptome of *Nonomuraea gerenzanensis* with new insights into its duplicated “magic” RNA polymerase. *Scientific reports* **6**, 18, <https://doi.org/10.1038/s41598-016-0025-0> (2016).
19. Marcone, G. L. *et al.* Novel mechanism of glycopeptide resistance in the A40926 producer *Nonomuraea* sp. ATCC 39727. *Antimicrobial agents and chemotherapy* **54**, 2465–2472, <https://doi.org/10.1128/AAC.00106-10> (2010).
20. Binda, E., Marcone, G. L., Pollegioni, L. & Marinelli, F. Characterization of VanYn, a novel D,D-peptidase/D,D-carboxypeptidase involved in glycopeptide antibiotic resistance in *Nonomuraea* sp. ATCC 39727. *The FEBS journal* **279**, 3203–3213, <https://doi.org/10.1111/j.1742-4658.2012.08706.x> (2012).
21. Sosio, M., Bossi, E., Bianchi, A. & Donadio, S. Multiple peptide synthetase gene clusters in Actinomycetes. *Molecular & general genetics: MGG* **264**, 213–221, <https://doi.org/10.1007/s004380000336> (2000).
22. Yushchuk, O. *et al.* Regulation of teicoplanin biosynthesis: refining the roles of *tei* cluster-situated regulatory genes. *Applied microbiology and biotechnology* **103**, 4089–4102, <https://doi.org/10.1007/s00253-019-09789-w> (2019).
23. Medema, M. H. *et al.* Minimum Information about a Biosynthetic Gene cluster. *Nat Chem Biol* **11**, 625–631, <https://doi.org/10.1038/nchembio.1890> (2015).
24. van der Heul, H. U., Bilyk, B. L., McDowall, K. J., Seipke, R. F. & van Wezel, G. P. Regulation of antibiotic production in Actinobacteria: new perspectives from the post-genomic era. *Natural product reports* **35**, 575–604, <https://doi.org/10.1039/c8np00012c> (2018).
25. Daniel-Ivadi, M., Pimentel-Elardo, S. & Nodwell, J. R. Control of Specialized Metabolism by Signaling and Transcriptional Regulation: Opportunities for New Platforms for Drug Discovery? *Annual review of microbiology* **72**, 25–48, <https://doi.org/10.1146/annurev-micro-022618-042458> (2018).
26. Nazari, B. *et al.* *Nonomuraea* sp. ATCC 55076 harbours the largest actinomycete chromosome to date and the kistamicin biosynthetic gene cluster. *MedChemComm* **8**, 780–788, <https://doi.org/10.1039/c6md00637j> (2017).

27. Gonsior, M. *et al.* Biosynthesis of the Peptide Antibiotic Feglymycin by a Linear Nonribosomal Peptide Synthetase Mechanism. *Chembiochem: a European journal of chemical biology* **16**, 2610–2614, <https://doi.org/10.1002/cbic.201500432> (2015).
28. Naruse, N., Oka, M., Konishi, M. & Oki, T. New antiviral antibiotics, kistamicins A and B. II. Structure determination. *The Journal of antibiotics* **46**, 1812–1818, <https://doi.org/10.7164/antibiotics.46.1812> (1993).
29. Naruse, N. *et al.* New antiviral antibiotics, kistamicins A and B. I. Taxonomy, production, isolation, physico-chemical properties and biological activities. *The Journal of antibiotics* **46**, 1804–1811, <https://doi.org/10.7164/antibiotics.46.1804> (1993).
30. Vertesy, L. *et al.* Feglymycin, a novel inhibitor of the replication of the human immunodeficiency virus. Fermentation, isolation and structure elucidation. *The Journal of antibiotics* **52**, 374–382, <https://doi.org/10.7164/antibiotics.52.374> (1999).
31. Kilian, R., Frasch, H. J., Kulik, A., Wohlleben, W. & Stegmann, E. The VanRS Homologous Two-Component System VnRSAb of the Glycopeptide Producer *Amycolatopsis balhimycina* Activates Transcription of the vanHAXSc Genes in *Streptomyces coelicolor*, but not in *A. balhimycina*. *Microbial drug resistance* **22**, 499–509, <https://doi.org/10.1089/mdr.2016.0128> (2016).
32. Foulston, L. & Bibb, M. Feed-forward regulation of microbisporicin biosynthesis in *Microbispora corallina*. *Journal of bacteriology* **193**, 3064–3071, <https://doi.org/10.1128/JB.00250-11> (2011).
33. Stegmann, E., Frasch, H. J., Kilian, R. & Pozzi, R. Self-resistance mechanisms of actinomycetes producing lipid II-targeting antibiotics. *International journal of medical microbiology: IJMM* **305**, 190–195, <https://doi.org/10.1016/j.ijmm.2014.12.015> (2015).
34. Alduina, R. *et al.* Expression in *Streptomyces lividans* of Nonomuraea genes cloned in an artificial chromosome. *Applied microbiology and biotechnology* **68**, 656–662, <https://doi.org/10.1007/s00253-005-1929-y> (2005).
35. Giardina, A. *et al.* Two heterologously expressed *Planobispora rosea* proteins cooperatively induce *Streptomyces lividans* thiostrepton uptake and storage from the extracellular medium. *Microbial cell factories* **9**, 44, <https://doi.org/10.1186/1475-2859-9-44> (2010).
36. Alt, S. *et al.* Toward Single-Peak Dalbavancin Analogs through Biology and Chemistry. *ACS Chem Biol* **14**, 356–360, <https://doi.org/10.1021/acscchembio.9b00050> (2019).
37. Gust, B., Challis, G. L., Fowler, K., Kieser, T. & Chater, K. F. PCR-targeted *Streptomyces* gene replacement identifies a protein domain needed for biosynthesis of the sesquiterpene soil odor geosmin. *Proc Natl Acad Sci USA* **100**, 1541–1546, <https://doi.org/10.1073/pnas.0337542100> (2003).
38. Donadio, S., Monciardini, P. & Sosio, M. Chapter 1. Approaches to discovering novel antibacterial and antifungal agents. *Methods in enzymology* **458**, 3–28, [https://doi.org/10.1016/S0076-6879\(09\)04801-0](https://doi.org/10.1016/S0076-6879(09)04801-0) (2009).
39. Gonzalez-Quinonez, N. *et al.* New PhiBT1 site-specific integrative vectors with neutral phenotype in *Streptomyces*. *Applied microbiology and biotechnology* **100**, 2797–2808, <https://doi.org/10.1007/s00253-015-7271-0> (2016).
40. Russo, M. *et al.* Binding abilities of polyaminocyclodextrins: polarimetric investigations and biological assays. *Beilstein journal of organic chemistry* **13**, 2751–2763, <https://doi.org/10.3762/bjoc.13.271> (2017).
41. Rubino, S. *et al.* Synthesis, structural characterization, anti-proliferative and antimicrobial activity of binuclear and mononuclear Pt(II) complexes with perfluoroalkyl-heterocyclic ligands. *Inorg Chim Acta* **483**, 180–190, <https://doi.org/10.1016/j.ica.2018.07.039> (2018).
42. Blin, K. *et al.* antiSMASH 5.0: updates to the secondary metabolite genome mining pipeline. *Nucleic acids research* **47**, W81–W87, <https://doi.org/10.1093/nar/gkz310> (2019).
43. Kumar, S., Stecher, G. & Tamura, K. MEGA7: Molecular Evolutionary Genetics Analysis Version 7.0 for Bigger Datasets. *Molecular biology and evolution* **33**, 1870–1874, <https://doi.org/10.1093/molbev/msw054> (2016).
44. MacNeil, D. J. *et al.* Analysis of *Streptomyces avermitilis* genes required for avermectin biosynthesis utilizing a novel integration vector. *Gene* **111**, 61–68, [https://doi.org/10.1016/0378-1119\(92\)90603-m](https://doi.org/10.1016/0378-1119(92)90603-m) (1992).
45. Datsenko, K. A. & Wanner, B. L. One-step inactivation of chromosomal genes in *Escherichia coli* K-12 using PCR products. *Proc Natl Acad Sci USA* **97**, 6640–6645, <https://doi.org/10.1073/pnas.120163297> (2000).

Acknowledgements

The authors thank Marta Aronica, Letizia Lo Grasso and Andrea Sabella (University of Palermo, Dep. STEBICEF) for their laboratory assistance and Anna Maria Puglia for precious discussion.

Author contributions

R.A. conceived, designed the work and wrote the manuscript. A.T. performed resistance assays and glycopeptide induction experiments, S.C. and C.F. performed transcriptional analysis and EMSA, P.C. performed protein analysis, M.S. carried out LC-MS analysis, S.D. performed bioinformatics analysis and wrote the manuscript. All authors contributed to the critical discussion of the manuscript, read and approved the final manuscript.

Competing interests

The authors declare no competing interests.

Additional information

Supplementary information is available for this paper at <https://doi.org/10.1038/s41598-020-63257-4>.

Correspondence and requests for materials should be addressed to R.A.

Reprints and permissions information is available at www.nature.com/reprints.

Publisher's note Springer Nature remains neutral with regard to jurisdictional claims in published maps and institutional affiliations.



Open Access This article is licensed under a Creative Commons Attribution 4.0 International License, which permits use, sharing, adaptation, distribution and reproduction in any medium or format, as long as you give appropriate credit to the original author(s) and the source, provide a link to the Creative Commons license, and indicate if changes were made. The images or other third party material in this article are included in the article's Creative Commons license, unless indicated otherwise in a credit line to the material. If material is not included in the article's Creative Commons license and your intended use is not permitted by statutory regulation or exceeds the permitted use, you will need to obtain permission directly from the copyright holder. To view a copy of this license, visit <http://creativecommons.org/licenses/by/4.0/>.

© The Author(s) 2020